Alkali/Silicate Interactions During Pulverized Coal Combustion

Neal Gallagher, Thomas W. Peterson and Jost Wendt, Chemical Engineering Department, University of Arizona, Tucson, AZ 85721.
Keywords: coal combustion, alkali, aluminosilicates, aerosols

Introduction

During the combustion of pulverized coal, inorganic ash constituents result in the formation of submicron aerosol and large ash particles. It is evident that chemical transformations involving this mineral matter plays an important role in the ultimate size distribution and chemical composition of these particles. One such mineral matter transformation mechanism suggested by data collected in this laboratory is reaction of sodium (or sodium containing species) with aluminosilicates. This observation led to the postulated mechanism of sodium mobilization within a burning char particle reacting with inherent aluminosilicate particles. Mobile sodium which reached the surface of the char particle was assumed to escape to the bulk flue gas environment. Previous work by Lindner and Wall (1988) however suggested that sodium reaction with aluminosilicates takes place primarily after the sodium escapes the char particle. This work attempts to determine the relative importance of sodium reaction with aluminosilicates inside and external to the char particle.

Experimental Work

Experimental facilities included a 17kW down-fired pulverized coal combustor which supported premixed self-sustained flames of pulverized coal. Fly-ash samples were extracted from the combustor and diluted with quench air using an isokinetic probe. Size segregation of the fly-ash samples was accomplished using a Mark II Andersen 1 ACFM cascade impactor. Impaction substrates were 0.2 μm Flouropore filters coated with polyethylene glycol 600 and the after-filter was an uncoated Flouropore filter. The size segregated samples were subjected to atomic absorbance for bulk elemental analysis at the University of Arizona and CCSEM analysis at the University of Kentucky.

Experiments were performed using numerous pulverized coal samples. The data reported herein represent results obtained from an Australian Coal (Loy Yang) and a North Dakota Lignite (Beulah). Loy Yang was chosen since it had a relatively high sodium to aluminosilicate ratio in the original coal, but overall low aluminosilicates (see Table I). In addition to conventional combustion experiments with this coal, experiments were conducted in which an aluminosilicate additive (94 g kaolinite per kg additive-free coal) was included in the coal feed. The kaolinite had a mass mean diameter of 0.5 μm, density 2.63 g/cm^3, and aerodynamic size of 0.81 μm. The purpose of these "doped" runs was to ascertain the effect on Na behavior of the aluminosilicate materials. Table I also shows the original ash analysis in addition to the calculated ash analysis for the doped coal experiments.

The results from the Loy Yang experiments in the absence of additive can be summarized by Figure 1. Here, the fraction oxide of the major elemental species is plotted as a function of the impactor collection plate. TF represents the Total Filter analysis, AF the after-filter analysis and Plates 1 to 8 the larger to smaller particle sizes for the aerodynamic cut-off diameter.

Enrichment of sodium in the smaller sizes is apparent. The sustantial fraction of the sodium found in the smaller sizes could be due to either surface condensation or homogeneous nucleation, but it is clear in either case that the fraction of species in the smallest size range might be indicative of the amount of Na that reached the vapor phase.

When the kaolinite additive is included, a substantial shift in the Na distribution with respect to particle size is witnessed (Figure 2). Not all Na has been taken up by the kaolinite, however, as attested by the large Na fraction still found in the after-filter. This result is not surprising, since it is likely that any remaining submicron aerosols will still be dominated by those species which most easily vaporize. In examining the cumulative mass fraction of the Na that appears on each stage, about 75% of the Na was found in a size range less than 0.65μm in the absence of additive. When kaolinite was included, that fraction fell to about 12%. The additive has significantly changed the overall sodium distribution, but it is still unclear as to whether the mechanism was due to increased condensation, or chemical reaction of the Na with the aluminosilicates.

The experiments with the Loy Yang were conducted because this coal has the rather unusual property of high Na fraction and low aluminosilicate fraction in the parent ash. The Beulah Lignite coal also has relatively high Na content, but contains silicate material in the form of quartz, kaolinite, illite, montmorillonite, mixed silicates and miscellaneous silicates. The Beulah lignite contains approximately 0.065 g Na/g silicates, whereas the doped Loy Yang contained 0.052 g Na/g silicates. Previous work done here showed that the lower the sodium to silicate ratio the higher the fraction of sodium captured. The fraction of sodium not captured was taken as the fraction found on impactor plate 8 and the after-filter (less than 0.65 μm). From this argument alone it would be expected that the doped Loy Yang would exhibit a lower fraction of sodium in a size range less than 0.65 μm than the Beulah Lignite. Figure 3 compares the cumulative fraction sodium oxide as a function of impactor plate for the Beulah Lignite and the doped Loy Yang experiments. These results suggest that because a fraction of the silicate-containing materials in the Beulah Lignite is included within the char matrix (as opposed to being entirely extraneous, as is the case with the kaolinite-doped Loy Yang), there is more efficient Na capture by the silicate materials.

Further examination of the Beulah lignite data also suggests that perhaps a pure condensation mechanism may not be sufficient to explain the behavior of the Na in the presence of the silicate-containing materials. Figure 4 plots the fraction of the impactor sample that is Na oxide vs. the inverse-square of the cut-off diameter. Under pure condensation, such a plot would yield a straight line. This is true for particles in the very small size ranges, but this behavior deviates for larger particles, in spite of the fact that there is a non-negligible amount of Na in these larger particles. Examination via CCSEM (these analyses were performed at the University of Kentucky) of the composition of the individual particles on the largest impactor plate (Plate 1, Figure 5) also shows that, while many of the aluminosilicate-bearing particles had essentially no Na in them, those that did contain Na did so in a fairly narrow range of Na-Al+Si compositions.

Finally, impactor samples collected by cascade impactor from later Loy Yang runs were analyzed in such a way as to try to separate those Na species which are chemically bound to the aluminosilicates from those which are simply surface-condensed on these particles. This was accomplished by dissolving a portion of the impactor sample in DI water (to get the surface-condensed sodium, presumably water soluble) and a portion in the standard acid reagant (to get all Na-containing species). There is some evidence that the reaction product of sodium with kaolinite (Punjak et al, 1989) is nephelite ($Na_2O{\cdot}Al_2O_3{\cdot}2SiO_2$). Nephelite is insoluble in cold water and decomposes in hot water. Our DI samples were never subjected to temperatures above 40 °C. Albite and jadite ($Na_2O{\cdot}Al_2O_3{\cdot}6SiO_2$ and $Na_2O{\cdot}Al_2O_3{\cdot}4SiO_2$) were also reported as insoluble. One possible product of reaction between sodium and quartz was $Na_2Si_2O_5$ as evidenced by equilibrium calculations. While this species is soluble, the amount of quartz in the Loy Yang was low overall.

The result of this analysis showed that while a large fraction of the Na captured was indeed water soluble (almost exclusively so in the smaller sizes), there was a substantial fraction of Na in the larger sizes (as high as 50% in some cases) which was water-insoluble. This certainly suggests that chemical reactions to form Na-aluminosilicates plays some role in the fate of Na during coal combustion.

Model Development

In order to mechanistically explain the varied experimental observations reported above, a model was developed to follow the release and capture of sodium species by Al and Si-bearing minerals. The model developed describes the release of sodium from a burning char particle, accounting for char particle shrinkage and sodium capture by silicate minerals, both within and outside the char particle. The assumed chemical reaction between sodium and alumino-silicates is based on work done by Punjak et. al (1989) and Uberoi et. al (1990). Additionally, chemical equilibrium calculations suggested the appropriate reaction to consider between sodium and quartz, the other form of Si considered.

Inside the char particle, species balances on the bound sodium, the "mobile" sodium and the included Si-containing species with which Na can react yield:

$$\frac{\partial C'_a}{\partial t} = D\frac{1}{r^2}\frac{\partial}{\partial r}\left(r^2\frac{\partial C'_a}{\partial r}\right) - C'_a\sum_{i=1}^{n}\frac{\eta_i k'_{ai} S_i k'_{mi} C'_i}{\eta_i k'_{ai} S_i C'_i + k'_{mi}} + k'_s C'_s \qquad 1$$

$$C'_a = 0 \text{ , } R = R_0 \quad at\ t = 0 \qquad 2$$

$$\frac{\partial C'_a}{\partial r} = 0 \qquad at\ r = 0 \qquad 3$$

$$-D\frac{\partial C_a'}{\partial r} = k_{mb}'(C_a' - C_b') \quad at\ r = R(t) \qquad 4$$

$$\frac{dC_s'}{dt} = -k_s'C_s' + \frac{C_s'R^{*3}}{(R^3 - R^{*3})}\frac{3}{R}\frac{dR}{dt} \qquad 5$$

$$C_s' = C_{s0}' \qquad at\ t = 0 \qquad 6$$

$$\frac{\partial C_i'}{\partial t} = -\frac{\beta_i \eta_i k_{ai}' S_i k_{mi}' C_i' C_a'}{\eta_i k_{ai}' S_i C_i' + k_{mi}'} - \frac{C_i'}{V}\frac{dV}{dt} \qquad 7$$

$$C_i' = f_i C_{i0}' \qquad at\ t = 0 \quad for\ i = 1,\ldots,n \qquad 8$$

Once the volatile migrates to the surface of the shrinking spherical char particle it can escape to the bulk flue gas phase. The concentration in the bulk, C_b', can change due to the mobile sodium escaping the char particle, reactions of the volatile species with extraneous silicate species j, particle shrinkage and concentration changes due to temperature effects. The condition given by equation 12 describes a bulk flue gas phase that is initially sodium-free.

$$\frac{dC_b'}{dt} = k_{mb}'a_v(C_a'|_{r=R} - C_b') - C_b'\sum_{j=1}^{n}\frac{\eta_j k_{aj}' S_j k_{mj}' C_j'}{\eta_j k_{aj}' S_j C_j' + k_{mj}'}$$

$$- (C_s' + C_a'|_{r=R})\frac{dR}{dt}a_v - \frac{C_b'}{V_b}\frac{dV_b}{dT}\frac{dT}{dt} \qquad 9$$

$$C_b' = 0 \qquad at\ \ t = 0 \qquad 10$$

Finally, a balance on the extraneous silicate species yields

$$\frac{dC_j'}{dt} = -\frac{\beta_j \eta_j k_{aj}' S_j k_{mj}' C_j' C_b'}{\eta_j k_{aj}' S_j C_j' + k_{mj}'} - \frac{C_j'}{V_b}\frac{dV_b}{dT}\frac{dT}{dt} \qquad 11$$

$$C_j' = g_j C_{j0}' \qquad at\ t = 0 \quad for\ j = 1,\ldots,n \qquad (12)$$

Parametric description of the reaction kinetics and mass transfer is accomplished with the following models:

$$k_{ai}' = A_i e^{-E_{ai}'/RT} \qquad (13)$$

$$k_{mb}' = D_b/R \qquad (14)$$

$$k_{mi}' = \frac{D_0 v}{R_i}\frac{4\pi R_i^2}{\frac{4}{3}\pi R_i^3}\frac{f_i C_{i0}'}{\rho_i} = \frac{3 v f_i C_{i0}'}{\rho_i}\frac{R_0^2}{R_i^2}\left(\frac{D_0}{R_0^2}\right) \qquad (15)$$

$$k_s' = A_s e^{-E_{as}/RT} \qquad (16)$$

$$\eta_{i,j} = 1. \qquad (17)$$

$$k_{mb}' a_v = \frac{D_{b0} v}{R}\left(a_{v0}\frac{R^2}{R_0^3 T}\right) = a_{v0}\frac{D_{b0}}{D_0}\frac{vu}{T}\left(\frac{D_0}{R_0^2}\right) \qquad (18)$$

$$k_{mj}' = \frac{D_{b0} v}{R_j}\frac{4\pi R_j^2}{\frac{4}{3}\pi R_j^3}\frac{g_j C_{j0}'}{\rho_j}\frac{298}{T} = \frac{D_{b0}}{D_0}\frac{3 v g_j C_{j0}'}{\rho_j}\frac{R_0^2}{R_j^2}\frac{298}{T}\left(\frac{D_0}{R_0^2}\right) \qquad (19)$$

$$a_v = \frac{(4\pi R^2)(feedcoal)}{(\rho_0 \frac{4}{3}\pi R_0^3)60(feedair)}\frac{298}{T} = a_{v0}\frac{R^2}{R_0^3 T} \qquad (20)$$

$$a_{v0} = \frac{(feedcoal)(298)}{\rho_0(20)(feedair)} \qquad (21)$$

The temperature was determined by fitting the four parameter model below to the measured temperature profile and residence time calculations.

$$T(t) = a_1(1 - e^{-a_2(t+a_4)})e^{-a_3(t+a_4)} \qquad 22$$

The residence time calculation accounted for geometry and temperature effects.

The char particle radius was determined using a simple char burnout model. According to Smith (1971) the rate of burnout R_{ac} is given by:

$$R_{ac} = Ae^{-E_a/RT_p} \qquad 22$$

Where R_{ac} is in grams of char per second per cm^2 external surface area per atmosphere oxygen. From this equation, the rate of change of particle radius is given by:

$$\frac{dR}{dt} = -\frac{p_{O_2}}{\rho_c}Ae^{-E_a/RT} \qquad 23$$

Where R is the char particle radius, and ρ_c is the char density.

Conclusions

Experiments suggest that the Na could escape the burning char and reach the bulk flue gas phase, as observed by the enrichment of Na in the smallest size classes. For the Loy Yang, the size distribution of the Na was greatly affected by the introduction of the additive, with the fraction of Na found in the smallest sizes being reduced from approximately 75% to 12%. It was clear that, while condensed Na species were dominant in the smaller particle size ranges, Na-containing aluminosilicates were indeed present in the large size particles.

Preliminary modeling results have indicated that (1) the reaction is fast enough for the Na to be captured by the included aluminosilicates during char burnout, and (2) the extent to which this occurs depends strongly on mass transfer of the Na through the char matrix.

REFERENCES

Lindner E.R. and Wall T.F., "An Experimental Study of Sodium-Ash Reaction During combustion of Pulverized Coal", Fourth Engineering Foundation Conference on Mineral Matter and Ash Deposition from Coal, Feb. 21-26, 1988, Santa Barbara, CA.

Punjak, W.A., Uberoi, M., and Shadman, F., "High Temperature Adsorption of Alkali Vapors on Solid Sorbents", AIChE Journal, **35**, 1186 (1989).

Smith, I.W., "Kinetics of Combustion of Size-Graded Pulverized Fuels in the Temperature Range 1200-2270 °K", Combustion and Flame, **17**, 303-314 (1971).

Uberoi, M., Punjak, W.A., and Shadman, F., "The Kinetics and Mechanism of Alkali Removal From Flue Gases by Solid Sorbents", Prog. Energy Combust. Sci. **16**, 205 (1990).

NOMENCLATURE

A_i = frequency factor for reaction of volatile with inherent silicate species i, 1/(cm^2 silicate i per g silicate i)/(g silicate i per cm^3 char)/(s).

A_j = frequency factor for reaction of volatile with extraneous silicate species j, 1/(cm^2 silicate j per g silicate)/(g silicate j per cm^3 flue)/(s).

A_s = frequency factor for release of bound volatile from the char matrix, (1/s).

A_v = char surface area per volume flue, (cm^2 char)/(cm^3 flue).

A_{v0}= reference parameter for A_v, (K).

C_a'= concentration of volatile inside the char particle,(g volatile)/(cm^3 char).

C_b'= concentration of volatile outside the char in the bulk flue gas phase, (g volatile)/(cm^3 char).

C_i'= concentration of inherent silicate species i, (g silicate i) /(cm^3 char).

C_j'= concentration of extraneous silicate species j, (g silicate j) /(cm^3 flue).

C_s'= concentration of volatile bound to the char matrix, (g bound vola- tile)/(cm^3 char).

C_{i0}'= initial concentration of all inherent silicate species,(g silicate)/(cm^3 char).

C_{j0}'= initial concentration of all extraneous silicate species, (g silicate)/(cm^3 flue).

C_{s0}'= initial concentration of volatile bound to the char matrix, (g bound volatile)/(cm^3 char).

D = effective diffusivity of volatile inside the char particle, (cm^2)/(s).

D_{ab}= diffusivity of volatile in a char particle pore, (cm^2)/(s).

D_b = diffusivity of volatile in the bulk flue gas phase, (cm^2)/(s).

D_{b0}= diffusivity of volatile in the bulk flue gas phase at the reference temperature T_0, (cm^2)/(s).

D_0 = effective diffusivity of volatile inside the char particle at the reference temperature T_0, (cm^2)/(s).

E_a = activation energy for char burning, (J/gmole).

E_{ai}= activation energy for reaction of volatile with inherent silicate species i, (J/gmole).

E_{aj}= activation energy for reaction of volatile with extraneous silicate species j, (J/gmole).

E_{as}= activation energy for release of bound volatile from the char matrix, (J/gmole).

f_i = fraction of inherent silicates that is species i.

g_i = fraction of extraneous silicates that is species j.

k_{ai}'= reaction rate coefficient between volatile and inherent silicate species i, 1/(cm^2 silicate i per g silicate i)/(g silicate i per cm^3 char)/(s).

k_{aj}'= reaction rate coefficient between volatile and extraneous silicate species j, 1/(cm^2 silicate j per g silicate j)/(g silicate j per cm^3 flue)/(s).

k_{mb}'= interphase mass transfer coefficient for transport of volatile from the char to the bulk flue gas phase, (cm)/(s).

k_{mi}'= interphase mass transfer coefficient for transport of volatile to inherent silicate species i, 1/(s).

k_{mj}'= interphase mass transfer coefficient for transport of volatile to extraneous silicate species j, 1/(s).

k_s'= reaction rate coefficient for release of volatile from the char matrix, 1/(s).

m = char particle mass, (g).

n = number of silicate species.

p_{O2}= partial pressure of oxygen, (atms).

r = radial position inside the spherical char particle, (cm).

R = char particle radius, (cm).

R_i = inherent silicate particle radius, (cm).

R_j = extraneous silicate particle radius, (cm).

R_0 = initial char particle radius, (cm).

R^* = final char particle radius (burnout complete), (cm).

S_i = specific surface area of inherent silicate species i, (cm^2 silicate i)/(g silicate i).

S_j= specific surface area of extraneous silicate species j, (cm^2 silicate j)/(g silicate j).

t = temporal variable, (s).

T = temperature, (K).

T_0 = reference temperature, (K).

V = char particle volume, (cm^3 char).

V_b = bulk flue gas volume, (cm^3 flue).

$\beta_{i,j}$ = stoicheometric factor, (g silicate i,j)/(g Na).

ϵ = char porosity, (cm^3 void)/(cm^3 char).

η_i = effectiveness factor for inherent silicate species i.

η_j = effectiveness factor for extraneous silicate species j.

ρ_i = inherent silicate density, (g)/(cm^3).

ρ_j = extraneous silicate density, (g)/(cm^3).

ρ_c = initial char particle density, (g)/(cm^3).

feedair = air feed rate into the combustor, (slpm).

feedcoal = coal feed rate into the combustor, (kg/hr).

Table I. Ash analysis for doped and undoped Loy Yang.

Loy Yang	undoped	undoped	doped	doped
oxides	% AR	frac oxide	% AR	frac oxide
Al_2O_3	0.04	0.036	3.36	0.404
SiO_2	0.16	0.132	4.02	0.483
CaO	0.06	0.047	0.05	0.006
Fe_2O_3	0.08	0.066	0.07	0.009
Na_2O	0.60	0.490	0.55	0.066
K_2O	< 0.01	0.004	< 0.01	0.001
MgO	0.28	0.225	0.25	0.030
Total	1.9	1.00	10.21	0.999

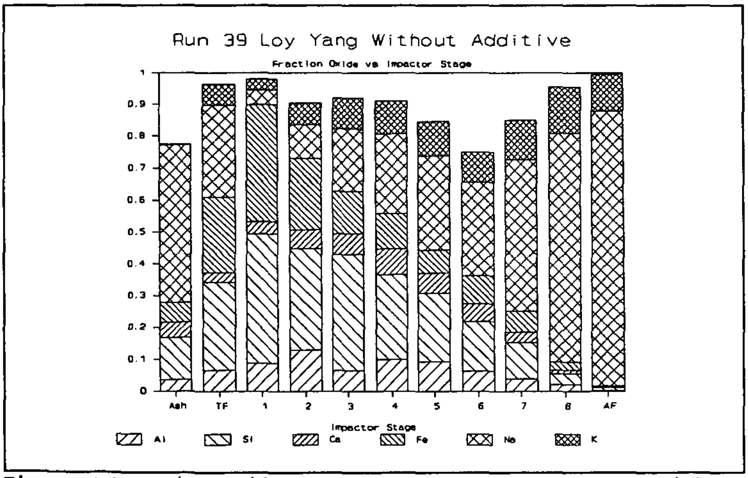

Figure 1 Fraction Oxide vs Impactor Stage for Loy Yang Without Additive

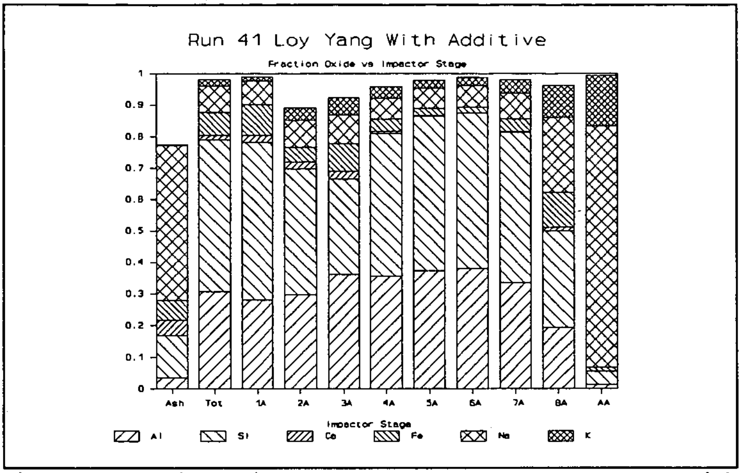

Figure 2 Fraction Oxide vs Impactor Stage for Loy Yang With Additive

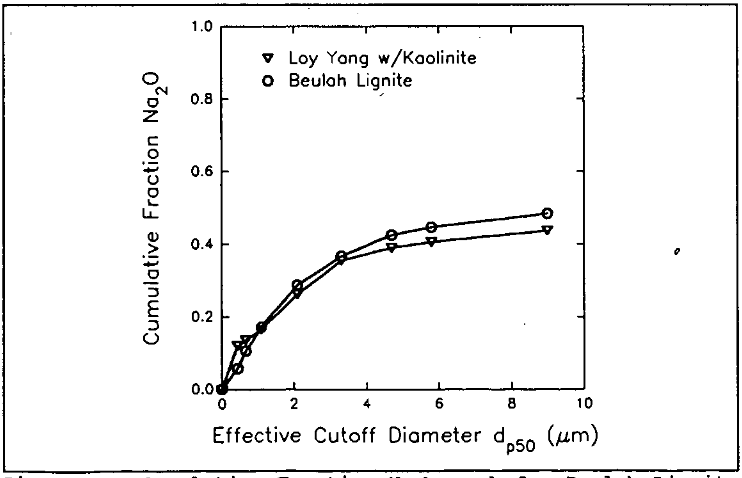

Figure 3. Cumulative Fraction Na_2O vs d_p for Beulah Lignite and Loy Yang doped with Kaolinite

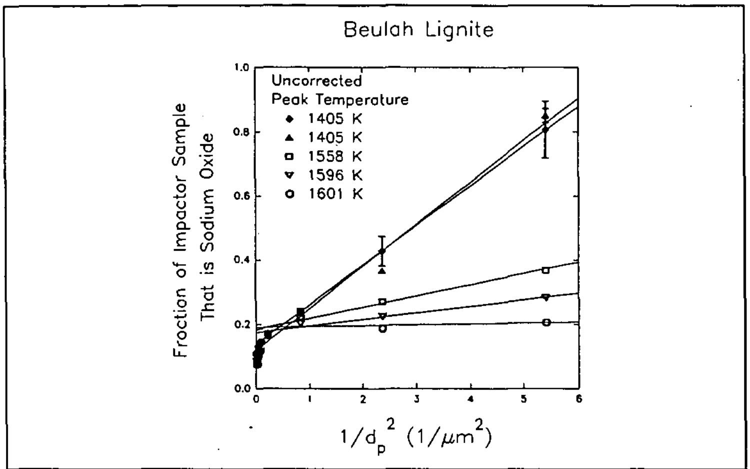

Figure 4 Fraction Na_2O vs $1/d_p^2$.

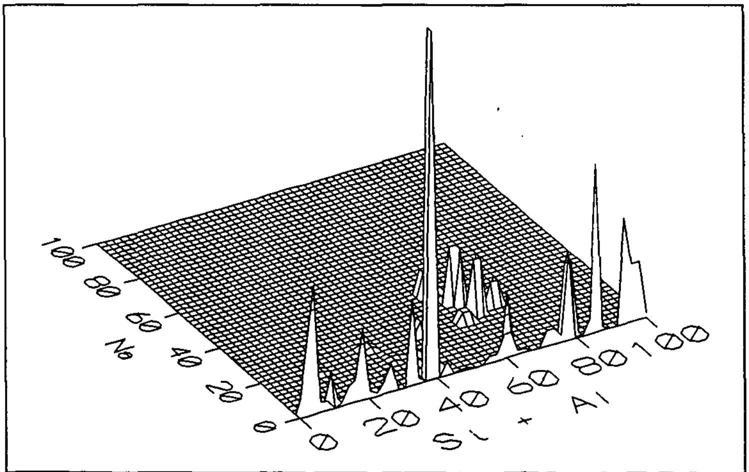

Figure 5. Beulah Lignite Impactor Plate 1.